



Picosecond intersubband dynamics in p- Si/SiGe quantum-well emitter structures

P. Murzyn, C. R. Pidgeon, J.-P. R. Wells, I. V. Bradley, Z. Ikonc, R. W. Kelsall, P. Harrison, S. A. Lynch, D. J. Paul, D. D. Arnone, D. J. Robbins, D. Norris, and A. G. Cullis

Citation: [Applied Physics Letters](#) **80**, 1456 (2002); doi: 10.1063/1.1452794

View online: <http://dx.doi.org/10.1063/1.1452794>

View Table of Contents: <http://scitation.aip.org/content/aip/journal/apl/80/8?ver=pdfcov>

Published by the [AIP Publishing](#)



Re-register for Table of Content Alerts

Create a profile.



Sign up today!



Picosecond intersubband dynamics in *p*-Si/SiGe quantum-well emitter structures

P. Murzyn, C. R. Pidgeon,^{a)} J.-P. R. Wells, and I. V. Bradley
Department of Physics, Heriot-Watt University, Edinburgh, EH14 4AS United Kingdom

Z. Ikonc, R. W. Kelsall, and P. Harrison
School of Electronic and Electrical Engineering, University of Leeds, Leeds, LS2 9JT United Kingdom

S. A. Lynch and D. J. Paul
University of Cambridge, Cavendish Laboratory, Madingley Road, Cambridge, CB3 0HE United Kingdom

D. D. Arnone
Toshiba Research Europe Ltd., 260 Science Park, Cambridge, CB3 0HE United Kingdom

D. J. Robbins
QinetiQ, St Andrews Road, Malvern, Worcs, WR14 3PS United Kingdom

D. Norris and A. G. Cullis
Department of Electronic Engineering, University of Sheffield, Sheffield, S1 3JD United Kingdom

(Received 18 October 2001; accepted for publication 16 December 2001)

We report time-resolved (ps) studies of the dynamics of intersubband transitions in *p*-Si/SiGe multi-quantum-well structures in the far-infrared (FIR) regime, $\hbar\omega < \hbar\omega_{LO}$, utilizing the Dutch free electron laser, (entitled FELIX—free electron laser for infrared radiation). The calculated scattering rates for optic and acoustic phonon, and alloy scattering have been included in a rate equation model of the transient FIR intersubband absorption, and show excellent agreement with our degenerate pump-probe spectroscopy measurements where, after an initial rise time determined by the resolution of our measurement, we determine a decay time of ~ 10 ps. This is found to be approximately constant in the temperature range from 4 to 100 K, in good agreement with the predictions of alloy scattering in the $\text{Si}_{0.7}\text{Ge}_{0.3}$ wells. © 2002 American Institute of Physics. [DOI: 10.1063/1.1452794]

p-type Si/SiGe quantum wells (QWs) are prospective candidates for intersubband (quantum cascade) lasers operating at mid- or far-infrared [(MIR) or (FIR)] wavelengths.¹ Possible advantages over other systems include the absence of polar optical phonons, the increased phonon energy in Si relative to most III–V materials, the existence of both the in-plane and *z*-polarized optical intersubband transitions [enabling vertical-cavity surface emission lasers (VCSELs)], and the low cost of material processing with the potential for on-chip integration. MIR emission,² and ultrafast time-resolved studies of the intersubband transitions,³ have been reported from this system, at photon energies greater than the optical phonon energy ($\hbar\omega > \hbar\omega_{LO}$). In the present work we report time-resolved studies of the dynamics of intersubband transitions in *p*-Si/SiGe multi-quantum-well structures in the FIR regime, $\hbar\omega < \hbar\omega_{LO}$, utilizing the Dutch free electron laser [Free Electron Laser for Infrared Radiation (FELIX)]. Although the ultimate aim of our program is to produce terahertz (THz) emitters in the VCSEL configuration, special transmitting prototype structures were designed and grown for the FELIX measurement of intersubband dynamics.

Our structures comprise ten modulation doped $\text{Si}_{0.7}\text{Ge}_{0.3}$ QWs with Si barriers, and $\text{Si}_{0.8}\text{Ge}_{0.2}$ buffers, on a $\text{Si}_{0.8}\text{Ge}_{0.2}$ virtual substrate. In the first sample (SQW2) the active layers were strain symmetrized on top of strain-relaxed nominally

$\text{Si}_{0.78}\text{Ge}_{0.22}$ buffers which involved growth of a ~ 3 - μm -thick linearly graded $\text{Si}_{1-x}\text{Ge}_x$ buffer followed by ~ 1 μm of $\text{Si}_{0.78}\text{Ge}_{0.22}$. Above the strain-relaxation buffer, ten periods of 5 nm *p*- $\text{Si}_{0.78}\text{Ge}_{0.22}$ ($N_A = 5 \times 10^{17} \text{ cm}^{-3}$ B), 2.8 nm *i*- $\text{Si}_{0.78}\text{Ge}_{0.22}$ spacer, 5.3 nm *i*-Si barrier, 12 nm *i*- $\text{Si}_{0.72}\text{Ge}_{0.28}$ quantum well, 5.3 nm *i*-Si barrier, 2.8 nm *i*- $\text{Si}_{0.78}\text{Ge}_{0.22}$ spacer, and 5 nm *p*- $\text{Si}_{0.78}\text{Ge}_{0.22}$ was grown. The wafer was capped with 100 nm $\text{Si}_{0.78}\text{Ge}_{0.22}$, 10 nm *p*- $\text{Si}_{0.78}\text{Ge}_{0.22}$, and 4.5 nm *i*-Si to reduce band bending at the surface. Layer thicknesses were measured by transmission electron microscopy, and the Ge mole fractions found by energy dispersive x-ray spectroscopy. In a second sample (SQW3) the structure comprised ten modulation doped, strain balanced $\text{Si}_{0.75}\text{Ge}_{0.25}$ quantum wells with Si barriers, grown on a $\text{Si}_{0.8}\text{Ge}_{0.2}$ virtual substrate, and separated by $\text{Si}_{0.8}\text{Ge}_{0.2}$ spacer regions.

The pump-probe measurements of nonradiative intersubband relaxation were made with FELIX in the temperature range 4–100 K. A three-beam balanced pump-probe technique described earlier⁴ was used in the FIR region of interest. The macropulse duration was 5 μs with 5 Hz repetition rate. The macropulse contained a train of micropulses of ~ 3 ps duration and 25 MHz repetition rate. A polarization rotator was used to change the polarization of the pump to be perpendicular to the probe, hence eliminating any so-called “coherence artifact” effect. Behind the sample an analyzer was placed to eliminate the scattered pump radiation from the detector.

^{a)}Electronic mail: c.r.pidgeon@hw.ac.uk

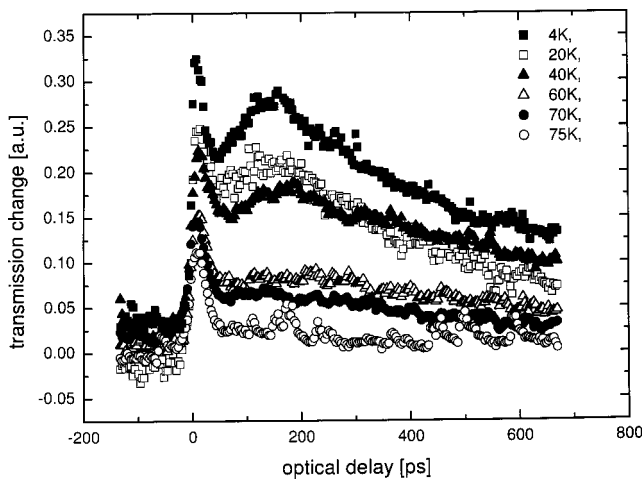


FIG. 1. Differential probe transmission vs optical delay for temperatures between 4 and 80 K at $\lambda=45 \mu\text{m}$ (sample SQW2) at oblique incidence (40°).

Measurements between 4 and 100 K were carried out at different angles of incidence, enabling access to both $LH1-HH1$ and $HH2-HH1$ transitions, in order to maximize the induced probe transmission signal change. The pump was set on the intersubband transition wavelength, obtained both from Fourier transform infrared (FTIR) transmission spectra and by maximizing the pump-probe transmission step. Degenerate pump-probe transmission spectra (i.e., differential probe transmission as a function of delay behind the bleaching pump pulse) are shown in Fig. 1 at $45 \mu\text{m}$, in the temperature range 4–80 K, for one of the two prototype structures measured (sample SQW2). In this case, in order to maximize the signal, the sample was set at an angle of 40° , accessing predominately $HH2-HH1$ transitions. But we note that the $HH2-HH1$ and $LH1-HH1$ transitions cannot be spectrally resolved for our structures at these long wavelengths, and must be distinguished by the experimental geometry and associated optical selection rules (see later).

These results are consistent with our theoretical calculations. Both SQW2 and SQW3 have FIR absorbing states localized in the spacer layers, in the energy range between the $HH1$ and $LH1$ quantum-well states, which are responsible for the dual-decay transmission response. The sharp feature with an exponential decay time of 10 ps, that remains at all temperatures, is associated with intersubband relaxation within the well. The slow subsequent rise and then fall of transmission, which occurs at low temperatures only, is associated with scattering into intermediate states confined in the spacer layers. Similar results were obtained on the second sample (SQW3), as shown in Fig. 2. The figures show the effect of both temperature and pump beam intensity on the transmission response, indicating the striking result that the sharp feature is relatively independent of both lattice and electron temperature. Finally, pump-probe experiments were performed on SQW2 for a range of pump wavelengths, confirming the resonance with the intersubband transition.

Electroluminescence emission spectra were previously obtained⁵ at both normal incidence ($LH1-HH1$ transitions) and in-plane (predominately $HH2-HH1$ transitions) by step-scan FTIR spectroscopy utilizing phase sensitive detection, the latter being observed only in TM polarization as

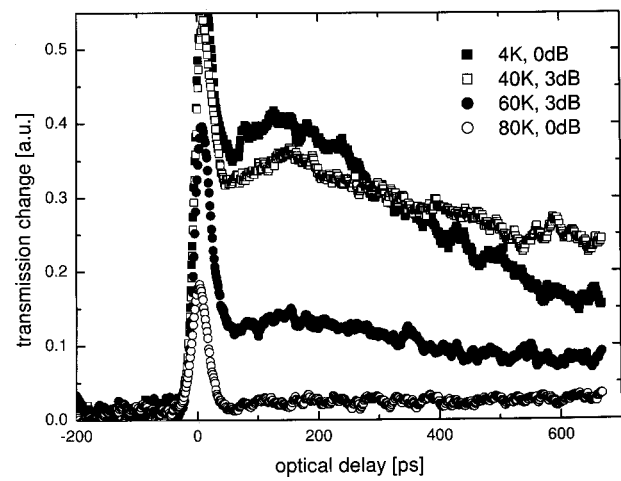


FIG. 2. Differential probe transmission vs optical delay for lattice temperatures of between 4 and 80 K, at $\lambda=52 \mu\text{m}$ (sample SQW3) at oblique incidence (45°). Note that, for the 40 and 60 K curves, the pump beam intensity is reduced by 3 dB relative to the 4 and 80 K traces.

expected. A periodic signal consisting of a train of square pulses with a 50% duty cycle and at a frequency of 418 Hz was injected into the sample, with the voltage drop in the plane of the quantum wells. FTIR spectra of the intersubband absorption were measured at the same time, in both configurations. A broad (full width at half maximum=15 meV) feature was observed centered on 28 and 24 meV for SQW2 and SQW3, respectively, in good agreement with our $\mathbf{k}\cdot\mathbf{p}$ calculations at these long wavelengths.⁵ Figure 3 shows the calculated energy minima for subbands up to quantum number 3 which are confined in the wells, and also for a further set of subbands which are confined in the unstrained SiGe spacer layers separating adjacent wells.

Calculations of intersubband relaxation rates due to phonon scattering by acoustic and the three optical phonon modes (Ge-Ge, Ge-Si, Si-Si), and due to alloy disorder scattering were performed for both $LH1-HH1$ and $HH2-HH1$ transitions with the fully anisotropic subband structure, obtained using the $6\times 6 \mathbf{k}\cdot\mathbf{p}$ method.^{5,6} The intersubband alloy scattering rates were calculated for a range of values of the alloy scattering potential U_0 reported in the literature,⁷ and the best agreement with our pump-probe experiments (later) was obtained with $U_0=0.3 \text{ eV}$ normalized to the primitive unit cell volume.^{5,7} It is found that in

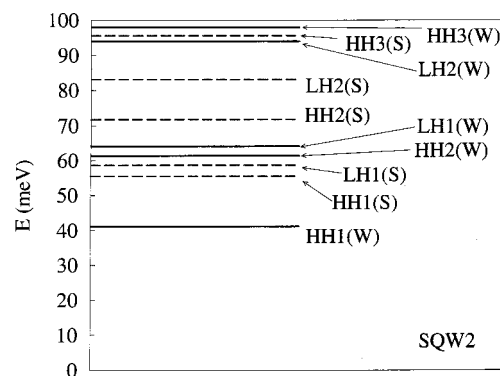


FIG. 3. Self-consistently calculated quantized hole states (subband energy minima) in sample SQW2, localized in the well (W) or spacer (S) layers. The spacer states are shown as dashed lines. The energy reference is the top of the valence band in the substrate (see Ref. 6).

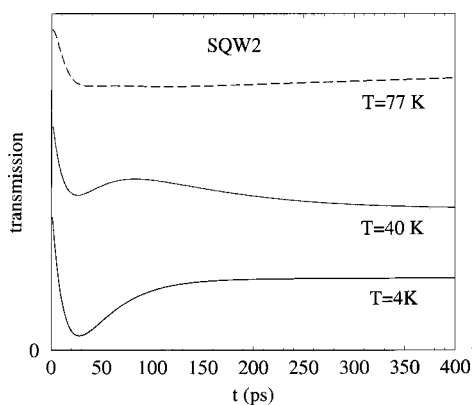


FIG. 4. Calculated differential probe transmission vs optical delay between pump and probe pulses for various temperatures for SQW2 at $45 \mu\text{m}$. The curves, which show the relative transmission, are shifted for clarity. The absolute transmission, which reduces with increasing temperature, is not shown here.

QWs with small transition energies (for THz emitters) and low temperatures, *intersubband* alloy scattering is by far the most important relaxation mechanism and acoustic phonon scattering is important only for the intrasubband carrier dynamics. This is by contrast with higher-energy QWs, however, where the optical phonon scattering prevails and a much shorter lifetime is determined.³

The calculated scattering rates for the intersubband transitions in the present bleaching experiment, including the relevant hole subband levels in both the quantum wells and the spacer layers, together with the absorption spectra for various subband populations, have been included in a rate equation model of the dynamic transmission, to give the overall computed pump-probe spectrum shown in Fig. 4 for several different temperatures. The starting condition at zero delay is taken as excitation of 50% of the total carrier population into higher lying subbands *within* the wells. However, the calculated transmission response was found to be relatively insensitive to the excitation level used. After the initial excitation, holes scatter back into both the *HH1* quantum well subband and the lowest spacer states (*LH1s* and *HH1s*). From the latter they can be reabsorbed to higher excited states causing further bleaching. The calculated lifetime for the principal transmission decay is ~ 10 ps, in good

agreement with experiment. The subsequent slow rise and fall in transmission, observed only at low temperature, is associated with scattering out of the FIR active spacer states—upon which the transmission recovers—and subsequent intrasubband relaxation within *HH1*, giving a transmission response which is again in good agreement with the experimental spectrum of Fig. 1.

In conclusion, intersubband relaxation in two strain-symmetrized *p*-Si/SiGe multiple quantum-well samples, both with subband energy separations less than the Si and Ge phonon energies, is found to be approximately constant in the temperature 4–100 K. The results are in good agreement with theoretical predictions, which indicate that *intersubband* alloy disorder scattering (which is almost temperature independent) is dominant in such structures throughout this temperature range. The intersubband lifetimes were also found to be insensitive to the FELIX pump power. These conclusions are in sharp contrast to similar measurements made by us on the GaAs/AlGaAs system in which polar optical phonon scattering dominates, giving a strong dependence of subband lifetime on both temperature and excitation level.^{8,9}

This Si/SiGe program is funded by DARPA on the USAF Contract No. F-19628-99-C-0074. The authors are grateful to EPSRC (UK) for support as part of the UK program at FELIX and are grateful for the skillful assistance of Dr. A. F. G. van der Meer.

¹L. Friedman, G. Sun, and R. A. Soref, Appl. Phys. Lett. **78**, 401 (2001).

²G. Dehlinger, L. Diehl, U. Gennser, H. Sigg, J. Faist, K. Ensslin, D. Grutzmacher, and E. Muller, Science **290**, 2277 (2000).

³R. A. Kaundl, M. Wurm, K. Reimann, M. Woerner, T. Elsaesser, C. Miesner, K. Vrunner, and G. Abstreiter, Phys. Rev. Lett. **86**, 1122 (2001).

⁴P. C. Findlay, C. R. Pidgeon, R. Kotitschke, A. Hollingworth, B. N. Murdin, C. J. G. Langerak, A. F. G. van der Meer, C. M. Ciesla, J. Oswald, A. Homer, G. Springholz, and G. Bauer, Phys. Rev. B **58**, 12908 (1998).

⁵Z. Ikonc, P. Harrison, and R. W. Kelsall, Phys. Rev. B **64**, 245311 (2001).

⁶S. Lynch, S. Dhillon, R. Bates, D. J. Paul, D. D. Arnone, D. J. Robbins, Z. Ikonc, R. W. Kelsall, P. Harrison, D. J. Norris, and A. G. Cullis, Proc. 2nd Int. Conf. on Silicon Epitaxy and Heterostructures, 2001.

⁷M. J. Kearney and A. I. Horrell, Semicond. Sci. Technol. **13**, 174 (1998).

⁸B. N. Murdin, W. Heiss, C. J. G. M. Langerak, S. C. Lee, I. Galbraith, G. Strasser, E. Gornik, M. Helm, and C. R. Pidgeon, Phys. Rev. B **55**, 5171 (1997).

⁹C. D. Bezzant, M. M. Chamberlain, H. P. M. Pellemans, B. N. Murdin, W. Batty, and M. Henini, Semicond. Sci. Technol. **14**, L25 (1999).